

Measurement of the $^{236}\text{U}(n, f)$ Cross Section in the Neutron Energy Range from 0.5 eV up to 25 keV

C. Wagemans,* L. De Smet, and S. Vermote

University of Gent, Department of Subatomic and Radiation Physics, B-9000 Gent, Belgium

J. Heyse† and J. Van Gils

*European Communities, Joint Research Centre, Institute for Reference Materials and Measurements
Retieseweg 111, B-2440 Geel, Belgium*

and

O. Serot

CEA-Cadarache, DEN/DER/SPRC/LEPh, F-13108 Saint Paul lez Durance, France

Received October 29, 2007

Accepted January 19, 2008

Abstract—The $^{236}\text{U}(n, f)$ cross section has been measured in the energy range from 0.5 eV to 25 keV at the Geel Electron Linear Accelerator neutron time-of-flight facility of the Institute for Reference Materials and Measurements in Geel, Belgium. A highly enriched ^{236}U sample was mounted back-to-back with a ^{10}B sample in the center of a Frisch-gridded ionization chamber, hence realizing a 2π detection geometry. A $^{235}\text{U}(n, f)$ cross-section control measurement was performed in the same experimental conditions. Special attention has been given to the fission resonance integral I_f and to the strongest resonance at 5.45 eV, for which a resonance analysis has been performed yielding $\Gamma_f = 1.7 \mu\text{eV}$. Both values are highly overestimated in the literature.

I. INTRODUCTION

Uranium-236 is produced by neutron capture in ^{235}U fuel, so neutron-induced reactions in ^{236}U influence the neutron balance of the fuel cycle. Moreover, the ^{236}U atoms contribute to the long-lived radioactivity of used fuel elements, and reprocessed uranium contains a non-negligible amount of ^{236}U . Hence, a decent knowledge of the $^{236}\text{U}(n, f)$ cross section is certainly desirable.

The experimental database for the $^{236}\text{U}(n, f)$ reaction cross section in the thermal and resonance region is very poor. Only one direct measurement with thermal neutrons is available, and the resonance data are scarce and discrepant:

1. Recently, Wagemans et al.¹ have performed the only direct thermal fission cross-section measurement at the high flux reactor of the Institute Laue-Langevin, yielding $\sigma(n_{th}, f) = (0.3 \pm 1) \text{ mb}$.

2. In 1970, Cramer and Bergen² made a first attempt to measure the $^{236}\text{U}(n, f)$ cross section from 35.2 eV to 2.935 MeV in the Pommard bomb shot experiment. They used a sample containing 0.15% of ^{235}U , but the data were not corrected for the corresponding important $^{235}\text{U}(n, f)$ contribution, so the small $^{236}\text{U}(n, f)$ resonances were lost in this background.

3. In 1972, Theobald et al.³ performed a measurement at the electron linear accelerator of the Central Bureau for Nuclear Measurements (CBNM), now the Institute for Reference Materials and Measurements (IRMM), in Geel, Belgium, covering the energy region from 5 to 415 eV. Fission neutrons were detected with a

*E-mail: cyrillus.wagemans@Ugent.be

†Current address: SCK•CEN, Boeretang 200, B-2400 Mol, Belgium

liquid scintillator, and signals due to neutrons and gamma rays were separated using the pulse-shape discrimination technique. The sample used contained 99.69% of ^{236}U and 0.199% of ^{235}U , which resulted in a strong $^{235}\text{U}(n,f)$ background. Their $\sigma_f(E)$ values are the only data set that has been released so far.

4. Also, the measurements by Parker et al.⁴ at the Los Alamos Neutron Science Center spallation neutron source suffered from a strong fission background since the samples used contained 0.3% of ^{235}U and 0.9% of ^{233}U . Because the main goal of these measurements was a study of the intermediate structure in the $^{236}\text{U}(n,f)$ cross section, no $\sigma_f(E)$ data set was released.

5. More recently, the $^{236}\text{U}(n,f)$ cross section has been measured at the n_TOF facility at CERN, Geneva, Switzerland,⁵ but final results have not been released so far.

In an effort to improve the database in the resonance region, experiments have been performed at the Geel Electron Linear Accelerator (GELINA) neutron time-of-flight (TOF) facility of the IRMM in Geel, Belgium, using a highly enriched ^{236}U sample.

II. EXPERIMENTAL PROCEDURE

II.A. Experimental Setup

The GELINA neutron TOF facility of the IRMM is the modernized electron linear accelerator of the CBNM, the main improvements being a reduction of the electron burst width from 10 to 1 ns and an increased neutron flux. At present, the linear accelerator delivers a pulsed and compressed electron beam that hits a rotating U target, hence producing bremsstrahlung gamma rays. These gamma rays create neutrons via (γ,n) and (γ,f) reactions. The neutrons are moderated in 4-cm-thick water-filled beryllium containers, resulting in a broad spectrum with energies ranging from a few milli-electron-volts up to a few mega-electron-volts. The shape of the moderated neutron spectrum can be approximated by a Maxwellian distribution at thermal energy with a $1/E$ high-energy tail. The energy of the neutrons is determined applying the TOF method.

A double Frisch-gridded ionization chamber with ultrapure methane as detector gas was installed at an 8.3-m-long flight path. The uranium sample (covered with a very thin polyimide foil to avoid contamination of the chamber by uranium alpha-decay recoils) was mounted in the center of the cathode, back-to-back with a ^{10}B layer. A schematic view of this setup is shown in Fig. 1. Two consecutive measurements were performed, one with a ^{236}U sample and a second one with a ^{235}U sample.

Each anode signal was amplified and sent to an analog-to-digital converter and a timing single-channel

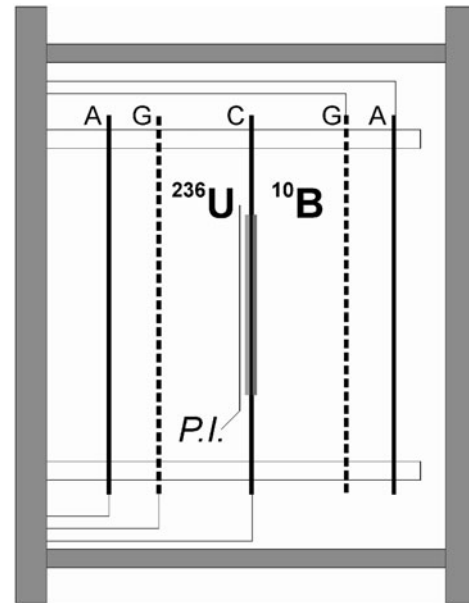


Fig. 1. Schematic layout of the Frisch-gridded ionization chamber. A, G, and C indicate anode, grid, and cathode, respectively. P.I. stands for polyimide foil.

analyzer (TSCA). The TSCA produces a fast logic signal T_n when the anode signal crosses a certain constant fraction of the pulse peak. Using a time coder, the TOF is determined by measuring the time between the start signal T_0 given by the linear accelerator at each electron burst and the stop signal T_n sent by the TSCA. The TOF value obtained in this way was stored in a LABVIEW-based data acquisition system together with the digitized anode pulse height for off-line analysis.

II.B. Samples

The uranium samples were prepared at the IRMM by electrolytic deposition of uranium oxide on a 20- μm -thick Al foil stretched on a metal frame. The active diameter was 50 mm. The isotopic enrichments and the layer thicknesses of the ^{236}U and ^{235}U samples used are summarized in Table I.

For the neutron flux determination, an evaporated elemental ^{10}B layer with an enrichment of 93%, a

TABLE I
Survey of the Uranium Sample Characteristics

Sample	Thickness ($\mu\text{g}/\text{cm}^2$)	Isotopic Composition (at.%)				
		^{233}U	^{234}U	^{235}U	^{236}U	^{238}U
^{235}U	110.9 ± 0.7	0.0056	0.0408	99.0402	0.2632	0.6502
^{236}U	209.9 ± 1.3			0.0043	99.9732	0.0225

thickness of $(8.05 \pm 0.10) \mu\text{g } ^{10}\text{B}/\text{cm}^2$, and a diameter of 50 mm was used. The amount of ^{10}B in the layer was determined in a dedicated measurement in a neutron beam, relative to the fission counting rate with a calibrated ^{235}U sample. Also, here the sample backing was a 20- μm -thick Al foil stretched on a metal frame.

H.C. Measurements

The $^{10}\text{B}(n, \alpha)^7\text{Li}$ reaction products (Fig. 2) and the $^{236}\text{U}(n, f)$ fragments were measured simultaneously with the double Frisch-gridded ionization chamber. In a control measurement, the ^{236}U sample was replaced by a ^{235}U sample with the same dimensions, maintaining the same cathode and ^{10}B sample. This permitted us to verify if the well-known $^{235}\text{U}(n, f)$ cross section was reproduced in our experiment. It also enabled correction for the small $^{235}\text{U}(n, f)$ contribution in the measurement with the ^{236}U sample (which contains 0.0043 at.% of ^{235}U ; see Table I) with $^{235}\text{U}(n, f)$ data of the same experimental resolution. Figure 3a shows the pulse-height spectrum for $^{235}\text{U}(n, f)$; Fig. 3b shows a typical $^{236}\text{U}(n, f)$ spectrum obtained in one of the runs. Because of the alpha activity of the ^{236}U sample combined with the 2π detection geometry, some alpha pileup was present, which was determined in a separate background measurement.

For all measurements, GELINA was operated at an 800-Hz repetition frequency, the electron pulses having a width of 1 ns. Overlapping neutrons from previous bursts were removed by a permanent cadmium overlap filter. The time-dependent background in the TOF spectra was determined by putting “black resonance” filters (Rh, Au, W, Co, and Mn) in the neutron beam.

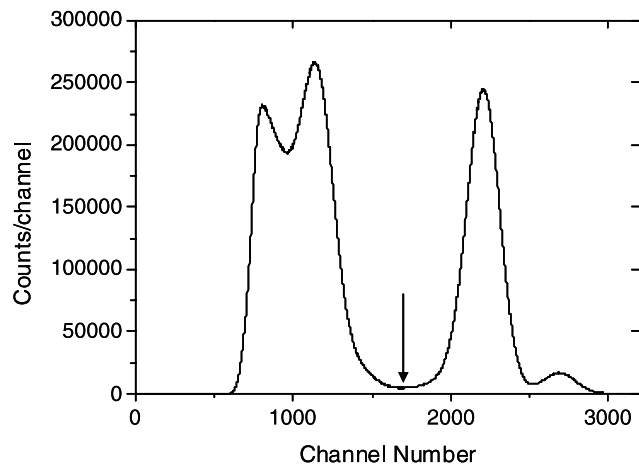


Fig. 2. Pulse-height spectrum of the $^{10}\text{B}(n, \alpha)^7\text{Li}$ particles. The arrow indicates the discrimination threshold.

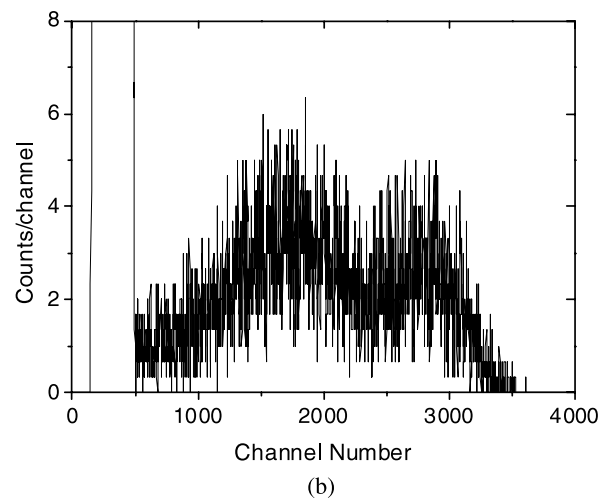
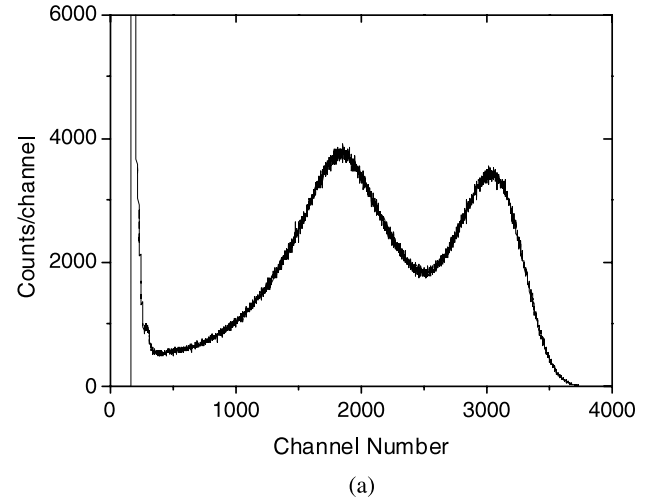


Fig. 3. (a) $^{235}\text{U}(n, f)$ pulse-height spectrum; (b) partial $^{236}\text{U}(n, f)$ pulse-height spectrum obtained in one of the runs.

III. RESULTS AND ANALYSIS

III.A. Data Analysis

In the measurements with the ^{236}U sample, both fission fragments are detected, so the fission counting rate Y_f is given by

$$Y_f(E_n) = \varepsilon_f [N_{6u} \sigma_{6u}(E_n) + N_{5u} \sigma_{5u}(E_n)] \varphi(E_n) + Y_f^{BGR}(E_n), \quad (1)$$

where

ε_f = detection geometry factor

N_{6u} = number of ^{236}U atoms in the ^{236}U sample

N_{5u} = number of ^{235}U atoms in the ^{236}U sample

- $\varphi(E_n)$ = neutron flux
- $\sigma_{6u}(E_n)$ = neutron-induced fission cross section for ²³⁶U
- $\sigma_{5u}(E_n)$ = neutron-induced fission cross section for ²³⁵U
- $Y_f^{BGR}(E_n)$ = TOF-dependent fission background.

Contributions due to the other U isotopes present in the sample are negligible.

With the discriminator setting used in the ¹⁰B(*n,α*)⁷Li measurement (see Fig. 2), only the alpha particles are detected; hence, the counting rate Y_B is given by

$$Y_B(E) = 2\varepsilon_B N_B \sigma_B(E_n) \varphi(E_n) + Y_B^{BGR}(E_n) \quad (2)$$

where

- ε_B = detection geometry factor
- N_B = number of ¹⁰B atoms in the ¹⁰B sample
- $\sigma_B(E_n)$ = ¹⁰B(*n,α*)⁷Li reaction cross section
- $Y_B^{BGR}(E_n)$ = TOF-dependent background in the ¹⁰B(*n,α*) measurement.

In both cases, the time-dependent background has been determined as a function of the TOF t by fitting a function $Y^{BGR}(t) = at^b + c$ through the counting rates in the black resonances and has been subtracted from the counting rates Y_f and Y_B . A typical example is given in Fig. 4, which shows the background in the black resonances of Mn.

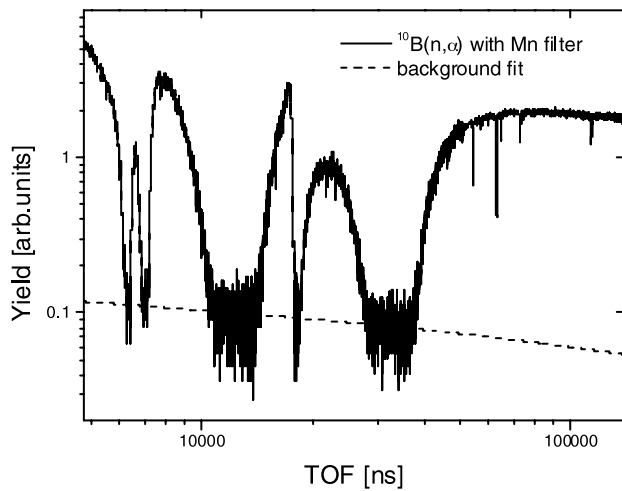


Fig. 4. Determination of the TOF-dependent background in the ¹⁰B(*n,α*) measurement with a Mn (black resonance) filter. The TOF region shown corresponds to neutron energies between 18 eV and 15.5 keV.

Dividing Eqs. (1) and (2) yields, after correction for the background,

$$\frac{Y_f(E_n) - Y_f^{BGR}(E_n)}{Y_B(E_n) - Y_B^{BGR}(E_n)} = \frac{\varepsilon_f}{2\varepsilon_B} \frac{N_{6u}\sigma_{6u}(E_n) + N_{5u}\sigma_{5u}(E_n)}{N_B\sigma_B(E_n)} \quad (3)$$

Since the detection geometry was 2π in both cases, $\varepsilon_f/\varepsilon_B = 1$; hence, the neutron-induced fission cross section of ²³⁶U can be calculated as follows:

$$\sigma_{6u}(E_n) = 2 \frac{N_B}{N_{6u}} \sigma_B^{\text{ENDF/B-VI}}(E_n) \frac{Y_f(E_n) - Y_f^{BGR}(E_n)}{Y_B(E_n) - Y_B^{BGR}(E_n)} - \frac{N_{5u}}{N_{6u}} \sigma_{5u}(E_n) \quad (4)$$

where $\sigma_B^{\text{ENDF/B-VI}}(E_n)$ is the ¹⁰B(*n,α*)⁷Li reference cross section adopted from the ENDF/B-VI evaluated data library.

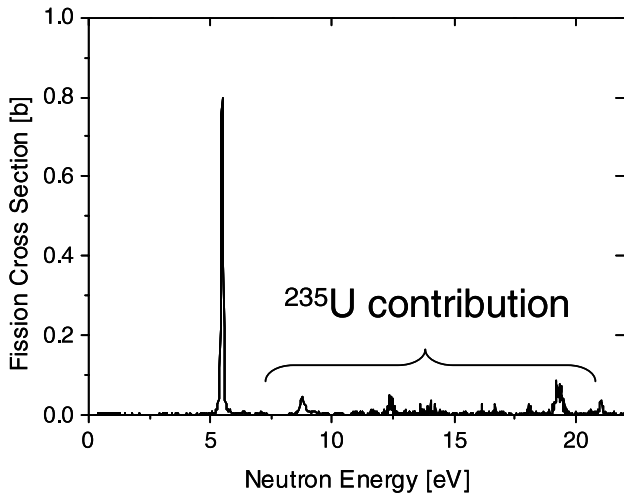
The ²³⁵U(*n,f*) cross section $\sigma_{5u}(E_n)$ in the last term of this expression was taken from the measurements with the ²³⁵U and ¹⁰B samples mentioned in Sec. II.C. In this way the raw ²³⁶U(*n,f*) data were corrected for the ²³⁵U(*n,f*) contribution due to the ²³⁵U impurities, maintaining the same energy resolution.

All these operations are implemented in the AGS computer code,⁶ which takes into account all sources of uncertainty and takes care of the error propagation, producing an experimental variance-covariance matrix. Apart from the counting statistics, the accuracy of the data is influenced by (a) an uncertainty of 1.2% on the number of ¹⁰B atoms, (b) an uncertainty of 0.6% on the number of atoms in the ²³⁶U and ²³⁵U samples, (c) the (small) uncertainty on the ¹⁰B(*n,α*)⁷Li reference cross section, (d) the uncertainty on the correction for the time-dependent background, and (e) the uncertainty on the correction for the ²³⁵U(*n,f*) contribution. Since the ²³⁵U(*n,f*) cross section is well known and because the ²³⁶U(*n,f*) and ²³⁵U(*n,f*) cross sections were measured under the same experimental conditions, the accuracy of this correction is mainly determined by the 2.3% accuracy on the ²³⁵U fraction in the ²³⁶U sample.

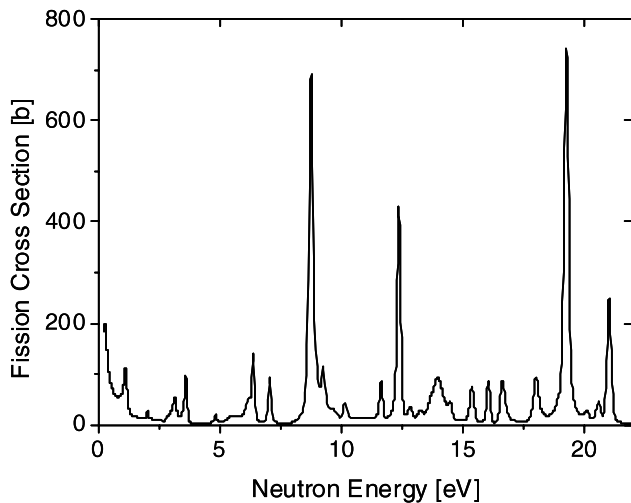
III.B. Results

Figure 5a shows the ²³⁶U(*n,f*) cross section in the neutron energy region from 0.5 to 22 eV before correction for the ²³⁵U(*n,f*) contribution. The corresponding ²³⁵U(*n,f*) cross section obtained in the ²³⁵U measurement under the same conditions is shown in Fig. 5b to demonstrate the importance and the quality of this correction.

Figure 6 shows the ²³⁶U(*n,f*) cross section in the neutron energy region from (a) 1 to 1000 eV and (b) 1 to



(a)



(b)

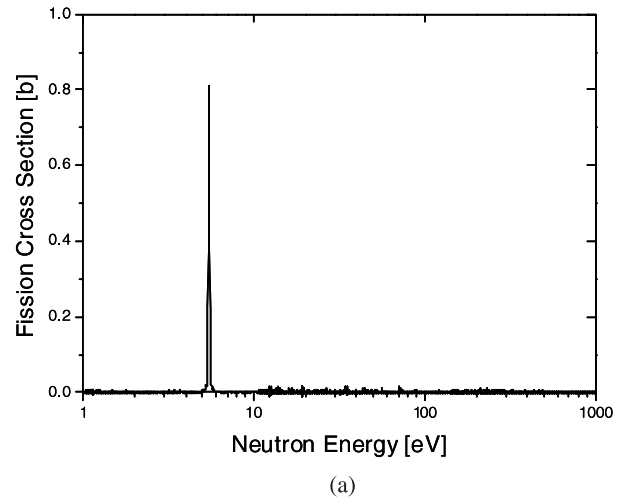
Fig. 5. (a) Raw $^{236}\text{U}(n,f)$ data uncorrected for the $^{235}\text{U}(n,f)$ contribution; (b) the corresponding $^{235}\text{U}(n,f)$ cross section.

25 keV after correction for the $^{235}\text{U}(n,f)$ contribution. Besides the dominant resonance at 5.45 keV, four resonance clusters with a spacing of ~ 3 keV can be observed, as reported by Parker et al.⁴ Because of the short flight path used in the present measurements, the resonances inside the clusters are not well resolved.

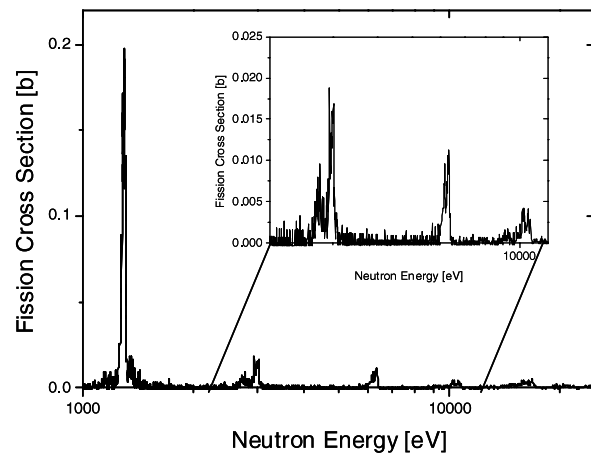
IV. DISCUSSION

IV.A. Intermediate Resonance Structure

The $^{236}\text{U}(n,f)$ cross-section results shown in Fig. 6 do not show the large number of resonances reported by



(a)



(b)

Fig. 6. The $^{236}\text{U}(n,f)$ cross section from (a) 1 to 1000 eV and (b) 1 to 25 keV.

Theobald et al.³ These resonances are probably due to a small sensitivity for radiative capture events of the liquid scintillator used in their measurements and/or an insufficient pulse-shape discrimination between gammas and neutrons. The present picture of fairly distant resonance clusters is a clear signature of intermediate structure, which is not surprising given the subbarrier character of the low-energy neutron-induced fission of ^{236}U .

IV.B. The 5.45-eV Resonance and the Thermal Region

Figure 7 shows the result of a fit to the present cross-section data in the region of the 5.45-eV resonance, using the SAMMY R-matrix code.⁷ With $\Gamma_\gamma = 24.5$ meV and $\Gamma_n = 2.16$ meV (as adopted in JEFF-3.1), a fission width $\Gamma_f = (1.7 \pm 0.1)$ μeV was obtained. This result is quite

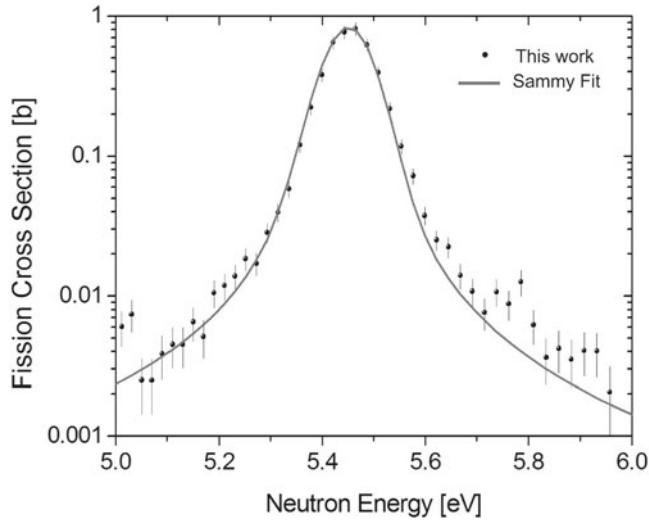


Fig. 7. SAMMY fit to the 5.45-eV resonance data points.

comparable with the value of $(1.3 \pm 0.1) \mu\text{eV}$ reported by Parker et al.,⁴ but it is two orders of magnitude lower than the value $\Gamma_f = 290 \mu\text{eV}$ adopted in JEFF-3.1. A Breit-Wigner extrapolation of the 5.45-eV resonance tail toward 0.0253 eV using the resonance parameters obtained in the present work yields a thermal contribution of $(0.22 \pm 0.02) \text{ mb}$ (Fig. 8), in agreement with the experimental thermal cross-section value of $(0.3 \pm 1) \text{ mb}$ of Wagemans et al.¹ For a good analytical description of the experimental (*n, γ*) cross section, the evaluated data files include a bound state (e.g., at -7.0 eV in JEFF-

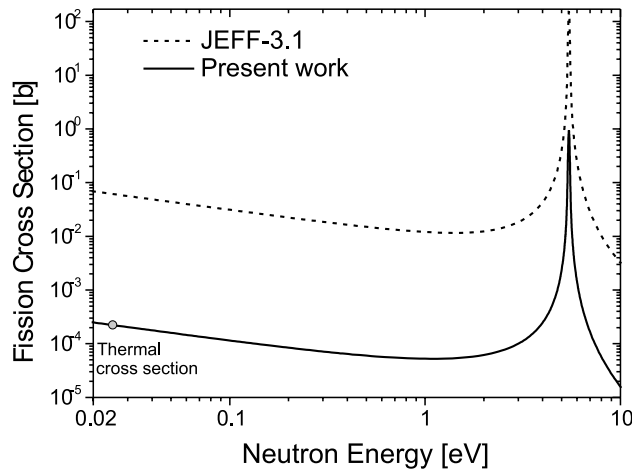


Fig. 8. Comparison of the JEFF-3.1 evaluation below 10 eV (intermittent line) with the present results extrapolated to the thermal energy region (full line) using SAMMY calculations.

3.1). If this bound state also has a fission component, this will lead to a small thermal contribution, which should be added to this 0.22 mb. The lower curve in Fig. 8 is an (extrapolated) result of the present measurements, which yield $\sigma_f(E)$ values about two orders of magnitude smaller than the corresponding JEFF-3.1 values (the same is true for JENDL-3.3 and ENDF/B-VII.0).

IV.C. The Fission Resonance Integral

In Table II, the values for the fission resonance integral

$$I_f = \int_{0.5 \text{ eV}}^{100 \text{ keV}} \sigma_f(E) \frac{dE}{E},$$

denoted by $I_f(100)$ in Table II, calculated from the JEFF-3.1, JENDL-3.3, and ENDF/B-VII.0 evaluated data libraries are reported. Since the ²³⁶U(*n,f*) cross-section data obtained in the present measurements only cover the neutron energy region from 0.5 eV to 25 keV, also the integral $I_f(25)$ being

$$I_f = \int_{0.5 \text{ eV}}^{25 \text{ keV}} \sigma_f(E) \frac{dE}{E}$$

has been calculated, which is almost equal to $I_f(100)$. The comparison in Table II clearly demonstrates that the fission resonance integrals calculated from all evaluated data libraries are too large by two orders of magnitude.

Also in Table II, the thermal neutron-induced fission cross sections adopted in the evaluated data libraries are reported and compared with the experimental value of Wagemans et al.¹ and with the value deduced above from a Breit-Wigner extrapolation of the 5.45-eV resonance as determined in the present work. Also here all evaluated data files report values that are too large by two orders of magnitude.

TABLE II

Comparison of the Thermal Fission Cross Section and the Fission Resonance Integral for ²³⁶U

Reference	$\sigma_f(\text{thermal})$ (mb)	$I_f(100)$ (b)	$I_f(25)$ (b)
ENDF/B-VII.0	47.1	4.460	4.452
JEFF-3.1	61.3	4.336	4.334
JENDL-3.3	61.3	4.363	4.359
Wagemans ¹	0.3 ± 1		
This work	$0.22^a \pm 0.02$		0.032 ± 0.001

^aBreit-Wigner extrapolation of the 5.45-eV resonance.

The comparisons in Table II clearly demonstrate that all three evaluated data libraries need to be corrected, since all of them are still relying on the wrong fission cross-section data of Theobald et al.³

V. CONCLUSION

In the present work, new experimental data for the $^{236}\text{U}(n, f)$ cross section are reported, showing a clear signature of intermediate structure. An R-matrix analysis has been performed of the dominant 5.45-eV resonance, yielding a fission width $\Gamma_f = (1.7 \pm 0.1) \mu\text{eV}$, much lower than the value of 290 μeV adopted in JEFF-3.1. All these new data are consistent with the experimental value for the thermal $^{236}\text{U}(n, f)$ cross section obtained at the high flux reactor of the Institut Laue-Langevin.¹ Both the results in the thermal and resonance region up to 25 keV are two orders of magnitude lower than those reported in the JEFF-3.1, JENDL-3.3, and ENDF/B-VII.0 evaluated data libraries, which should be revised.

REFERENCES

1. C. WAGEMANS, O. SEROT, P. GELTENBORT, and O. ZIMMER, "Experimental Determination of the $^{236}\text{U}(n_{th}, f)$ Cross Section," *Nucl. Sci. Eng.*, **136**, 415 (2000).
2. J. CRAMER and D. BERGEN, LA-4420, p. 74, Los Alamos National Laboratory (1970).
3. J. THEOBALD, J. WARTENA, H. WEIGMANN, and F. POORTMANS, *Nucl. Phys. A*, **181**, 639 (1972).
4. W. PARKER, E. LYNN, G. MORGAN, P. LISOWSKI, A. CARLSON, and N. HILL, *Phys. Rev. C*, **49**, 672 (1994).
5. U. ABBONDANNO et al., *AIP Conf. Proc.*, **769**, 724 (2005).
6. C. BASTIAN, A. BORELLA, F. GUNSING, J. HEYSE, S. KOPECKY, G. NOGUERE, P. SIEGLER, and P. SCHILLENBEECKX, "AGS, A Computer Code for Uncertainty Propagation in Time-of-Flight Cross Section Data," *Proc. PHYSOR-2006*, Vancouver, Canada, September 10–14, 2006, American Nuclear Society (2006) (CD-ROM).
7. N. LARSON, ORNL/TM-9179/R6 ENDF-364, Oak Ridge National Laboratory (2003).